Magnetic torque enhanced by tunable dipolar interactions

C. Pellet-Mary , P. Huillery, M. Perdriat, and G. Hétet

Laboratoire de Physique de l'École Normale Supérieure, École Normale Supérieure, PSL Research University, CNRS, Sorbonne Université, Université de Paris, 24 rue Lhomond, 75231 Paris Cedex 05, France

We use tunable dipolar interactions between the spins of nitrogen-vacancy (NV) centers in diamond to rotate a diamond crystal. Specifically, we employ cross-relaxation between the electronic spin of pairs of NV centers in a trapped diamond to enhance the anisotropic NV paramagnetism and thus to increase the associated spin torque. Our observations open a path towards the use of mechanical oscillators to detect paramagnetic defects that lack optical transitions, to the investigation of angular momentum conservation in spin relaxation processes, and to different means of cooling the motion of mechanical oscillators.

Controlling the motion of macroscopic oscillators at ultralow motional temperatures has been the subject of intense research over the past decades. In this direction, optomechanical systems, where the motion of micro-objects is strongly coupled to laser light, have had tremendous success [1]. Similar interaction schemes are propounded in order to strongly couple long-lived atomic spins, such as the electronic spin of nitrogen-vacancy (NV) centers in diamond, to mechanical oscillators [2–4]. At the single spin level, this achievement would offer the formidable prospect of transferring the inherent quantum nature of electronic spins to the oscillators, with foreseeable far-reaching implications in quantum sensing and tests of quantum mechanics [5–7].

Most efforts using single NV centers are presently hampered by their low coupling strengths to the motion, which are currently far below typical spin decoherence rates [8–11]. One solution to counteract this issue is to work with large ensembles of spins [10]. This approach does not lend itself easily to observing nonlinear spin-mechanical effects, but may offer a more favorable path towards ground state spin cooling [3] and would enable the observation of many-body effects mediated by the motion [7,12].

However, although the spin-mechanical coupling strength is predicted to increase linearly with the number of spins, this scaling law is modified when the mean distance between the atomic defects is of the order of 10 nm because of dipolar interactions. Dipolar interactions can significantly enrich the physics at play and have, for instance, been employed in the optical domain to increase the coupling of electron dipoles to mechanical motion, akin to superradiant processes [13–16]. Further, using NV centers, the coupling strength can be tuned resonantly among different NV orientations [17], offering prospects for studying the interplay between dipolar interactions and motional degrees of freedom in a controlled fashion. Increasing the density of NV centers also means that they can couple more efficiently to other spins in the diamond [18–21] and even transfer their polarization [22]. Angular momentum exchange in such cross-relaxation processes could result in a rotation of the crystal, as in the Einstein–de Haas effect, and

even enable controlling mechanical oscillators in the quantum regime [23].

Here, we employ resonant dipolar interactions between NV centers to rotate a micromechanical oscillator. Specifically, we use NV centers inside a diamond that is levitating in a Paul trap and use resonant cross-relaxation (CR) between them to observe a spin torque coming from the NV paramagnetism. The mechanism is described in Fig. 1. As depicted in the left panel, NV centers are found in four different orientations in the diamond crystalline structure. In the presence of an external magnetic field at an angle with respect to the NV axis, NV centers acquire a magnetization. Due to quasirotational invariance of the problem, although each NV class could exert a significant magnetic torque to the diamond, the total spin torque τ_s is reduced. The NV paramagnetic susceptibility is then only on the order of the diamagnetism coming from the orbital motion of the electrons in the diamond valence band. The key point of our study is that resonant dipole-dipole interactions between the spin of NV centers of different orientations can be enhanced which, in turn, increases the paramagnetism.

Let us now describe how resonant dipole-dipole interactions can be harnessed. When the electronic spin transitions of NV centers become resonant, the polarization of the NV of different orientations can be exchanged through cross-relaxation [24]. The conditions on the magnetic field for CR to occur are described in Sec. I of the Supplemental Material (SM) [25]. The right panel of Fig. 1 shows a CR mechanism that partly removes the contribution from two classes of NV centers (labeled 1 and 3 in Fig. 1), which breaks the four-spin rotational invariance. The total spin torque τ_s can then be large enough to rotate the diamond. The ingredient that enables such CR to take place is the differing T_1 from one NV to another. It was shown in Ref. [30] that in highly doped diamond samples, a few fast-decaying NV centers, so-called *fluctuators*, can then depolarize an ensemble of NV centers through dipolar interaction. Figure 2(b) depicts the dipolar interaction between two NV centers. In this example, the electronic spin of NV_1 is polarized in the ground state via the
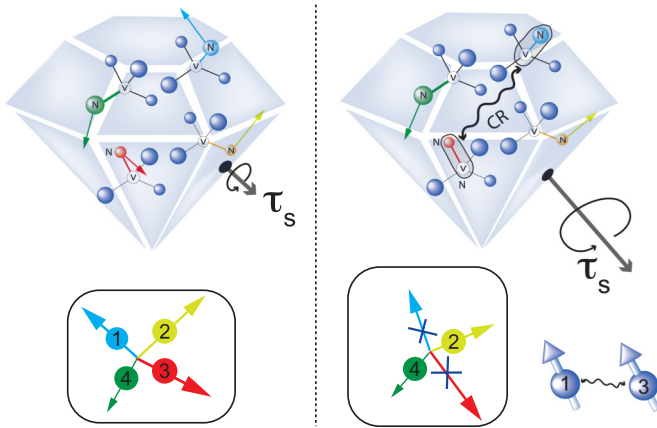
FIG. 1. General principle of the resonant dipole-dipole enhanced mechanical rotation. The four possible directions of the nitrogen-vacancy centers in the diamond are shown in the left/right panels together with their spin-torque contributions (arrows of the corresponding colors). Left panel: The (quasi)rotational invariance gives a small total spin torque τ_s. Right panel: A magnetic field (not shown) is tuned so that the energy levels of the spin classes 1 and 3 become degenerate. Cross-relaxation (CR) between these two classes of NV centers occurs, altering the rotational symmetry and increasing τ_s.

green laser, whereas NV_2 is a fluctuator, which has a shorter relaxation time T_1 than the polarization time. The spins will exchange magnetic quanta through flip-flop processes resulting in a depolarization of NV_1. This was shown to reduce the average T_1 of the ensemble from the phonon-limited T_1 ($\approx$ ms) to a few hundreds of microseconds [31] and to lower the total photoluminescence (PL) [17,18,30,32–37] in bulk materials. The origin of the fast-decaying NV centers was attributed to the presence of charge tunneling among closely packed NV centers [30]. The NV centers that undergo tunneling with other impurities (possibly with the substitutional nitrogen defect [38]) have a largely reduced longitudinal spin lifetime T_1.

Such a process has yet to be studied in detail with nano- or microparticles. Smaller diamond particles in fact tend to suffer from extra parasitic surface effects such as spin depolarization due to an interaction with paramagnetic dangling bonds on the surface [39], or enhanced charge transfer between the NV^0 and NV^- charge states [40], so it is essential to verify that it can be observed with microparticles. We start by searching for CR using microdiamonds that are physically attached to the trap, by employing a fixed bias magnetic field $||\mathbf{B}_{bias}|| \approx 100$ G and by tuning another magnetic field $\mathbf{B}_{em}$ at some angle with respect to $\mathbf{B}_{bias}$ using an electromagnet [see Fig. 2(a)]. The change in orientation of the total magnetic field can be visualized in Sec. I of the SM [25].

The photoluminescence from the NV centers is detected using standard confocal microscopy. At specific magnetic field directions with respect to the crystalline axes, degeneracy between the spin of NV centers can be reached [17]. We measured the T_1 time in these conditions by applying a green laser that polarizes the NV centers and measure the photoluminescence at a later time. Such a measurement can be significantly impacted by the recharging of NV centers in the dark [30,36,41,42]. In order to accurately measure the T_1
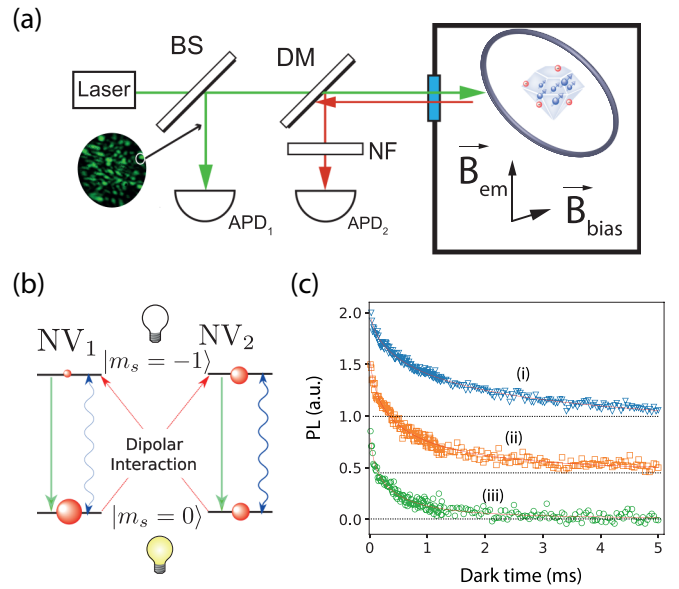

FIG. 2. Schematics of the experiment. A microdiamond is levitating in a ring Paul trap enclosed in a vacuum chamber. A green laser is used both to polarize the NV centers in the levitating diamond and to detect the angular motion. Part of the speckle pattern formed in the image plane is sent onto avalanche photodiode APD_1 after passing through a beam splitter (BS). The photoluminescence from the NV centers is collected on APD_2 after filtering out the green laser light by a dichroic mirror (DM) and a notch filter (NF). (a) Sketch showing the NV-NV cross-relaxation process. Green arrows represent the optical pumping to the brighter $|m_s = 0\rangle$ state. The two curvy blue arrows with different thicknesses represent the short/long longitudinal relaxation of NV_2/NV_1. Red circles represent the population in each state and red dashed arrows represent the resonant dipole-dipole interaction between the two NV centers. (c) Measurements of the longitudinal relaxation from a single NV class when (i) it is not resonant with any other classes ($T_1 = 1.61$ ms), (ii) when it is resonant with another class ($T_1 = 490$ μs), and (iii) when it is resonant with the three other classes ($T_1 = 220$ μs). The three traces have been offset for clarity.

and remove the changing PL due to the recharging effects, we use the sequence presented in Sec. III of the SM [25], where a microwave pulse is or is not applied prior to spin relaxation. The PL signals acquired in the two different measurements are then subtracted and shown for different degeneracy configurations in Fig. 2(c). In the absence of degeneracy, we observe a profile that is close to a stretched exponentially decaying curve [30], from which we extract a $T_1 = 1.61$ ms, already shorter than the phonon-limited lifetime in dilute bulk materials [39]. This lifetime is even further reduced when more orientations are brought to resonance. This hints at the role played by dipolar interactions, which are enhanced when more classes of NV centers are resonant [17,30].

The main goal in the present Letter is to demonstrate mechanical action of such dipolar-induced relaxations when diamonds are levitating in the Paul trap. One major extra ingredient for this is the magnetization of the NV centers when they are laser polarized. Let us consider first the dependence of the ground state energy of a single spin as a function of the angle between a magnetic field and the NV axis. The Hamiltonian for one NV orientation with quantization axis z'
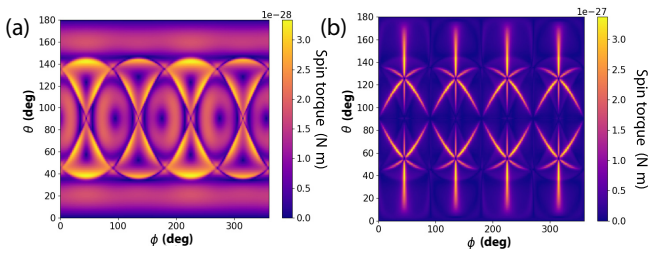
FIG. 3. Numerical simulations of the spin torques on a diamond containing one NV center per orientation as a function of θ and ϕ, the polar and azimuthal angle with respect to the [100] direction. (a) and (b) show the torque without and with cross-relaxation between NV centers respectively. Notice the different torque scales.

in the particle frame reads

$$\hat{H}_{NV} = \hbar D \hat{S}_{z'}^2 + \hbar \gamma_e \mathbf{B} \cdot \hat{\mathbf{S}}, \qquad (1)$$

where $\hat{\mathbf{S}}$ is the spin vector, $D = (2\pi)2.87$ GHz the zero-field splitting, and $\mathbf{B}$ is the external magnetic field. Under the condition $\gamma||\mathbf{B}|| \ll D$, assuming an NV center in the (x, z) plane and a B field along z, $\hat{H}_B = \hbar \gamma_e \mathbf{B} \cdot \hat{\mathbf{S}} = \hbar \gamma_e B(\hat{S}_{x'} \sin\theta + \hat{S}_{z'} \cos\theta)$ can be treated as a perturbation to the anisotropic part $\hbar D \hat{S}_{z'}^2$ of the Hamiltonian. Here, θ is the angle between the magnetic field and the body-fixed NV center axis. The energy ϵ_g of the ground state perturbed by the B field is then

$$\epsilon_g = \sum_{m_s=\pm 1} \frac{|\langle 0|\hat{H}_B|\pm 1\rangle|^2}{-\epsilon_{\pm 1}^0} = -\hbar \frac{(\gamma_e B_\perp)^2}{D}, \qquad (2)$$

where $B_\perp = B\sin\theta$. A direct use of the Hellmann-Feynman theorem can give the torque in the ground state. We find that

$$\tau_s = -\frac{\partial \epsilon_g}{\partial \theta} = \hbar \frac{(\gamma_e B)^2}{D} \sin 2\theta. \qquad (3)$$

A proof of the applicability of this theorem in the presence of dissipation is presented in Sec. IV of the SM [25]. At an angle $\theta = \pi/4$, where the torque is maximized and at a B field of 100 G, we obtain $\tau_s \approx 2 \times 10^{-27}$ N m. Taking into account the whole NV level structure, we then find $\tau_s \approx 10^{-18}$ N m, using 10^9 spins polarized in the ground state. Taking a librational confinement frequency of the diamond in the Paul trap to be around $\omega_\theta/(2\pi) \approx 1$ kHz, we obtain a spin-torque-induced angular displacement of $\tau/I_y\omega_\theta^2 \approx 1$ mrad, which can be measured with a high signal-to-noise ratio in our setup [10]. Here, $I_y \approx 10^{-22}$ kg m^2 is the moment of inertia of the particle around the y axis.

As already hinted at, however, the contributions from the other NV classes must also be taken into account (see Fig. 1). Figure 3 presents the result of numerical calculations of the torque coming from the four classes of NV centers, assuming only one NV per orientation here. Figure 3(a) shows the torque magnitude as a function of θ and ϕ without taking into account CR. The torque from each of the four classes appears clearly from the symmetry. Their different contributions however sum up to give a maximum torque of around 10^{-28} N m, which is 20 times smaller than the torque that can be obtained for a single class. The quasirotational invariance of the problem thus hinders the diamond paramagnetism. When two classes of NV center are resonant, however, the induced

cross-relaxation partly breaks this rotational invariance. Figure 3(b) shows the same plot, but including CR. Details on the model can be found in Sec. VI of the SM [25]. Here, we use numbers that are deduced from the experimental observations of the CR-induced change of the T_1 in Fig. 2(b). One can see that a new pattern with a larger spin torque is superimposed onto the previous map. These larger values coincide with crossings of the crystal planes where NV degeneracies occur. At these coordinates, one recovers the torque estimation of Eq. (3), found for a single class, which would then imply a spin torque that overcomes the Paul trap confinement.

To observe the effect of such resonant dipolar interactions on the motion, we use similar parameters and magnetic field arrangement than when the diamonds were not levitating. The diamond crystalline direction with respect to the magnetic field direction is characterized by recording mechanically detected magnetic resonances (MDMRs) [10] similar to in magnetic resonance force microscopy (MRFM) [43]. The angular motion is detected by collecting the back-reflected green light from the diamond interface [see Fig. 2(a)], separated from the excitation light using a beam splitter as a microwave drives the spin to the $m_s = -1$ state. Figure 4(a) shows MDMR detection of spin resonances for three different $\mathbf{B}_{em}$ amplitudes. At 10 and 25 G, one can observe four peaks in the spectrum that demonstrate a microwave-induced torque on the diamond from the four classes of NV centers. At 17 G, however, two classes merge at a microwave frequency of 2.75 GHz. This is where we expect to observe CR.

A detailed analysis developed in Sec. I of the SM [25] suggests that since we observe a single degeneracy at 17 G, the magnetic field crosses a plane that is perpendicular to the [110] direction, as shown in Fig. 4(a). Figure 4(b) shows the photoluminescence as a function of $\mathbf{B}_{em}$ both experimentally [trace (i)] and numerically [trace (ii)]. As expected, the PL decreases across the degeneracies at around the same magnetic field value. Figure 4(c)(i) is a measurement of the diamond angular position acquired using the reflected green laser, simultaneously to the PL. In the linear regime, the detected reflected laser intensity is proportional to the angular deviation. Calibration of the absolute angular deviation would require knowledge of the angles between the NV centers and the diamond main axes [10].

Trace (ii) is the corresponding calculation. A pronounced variation of the reflected signal is also observed, demonstrating the close correspondence between degeneracy and diamond rotation, and the enhanced spin torque as the dipolar interactions between the spins increase. Note that, as opposed to the PL detection which always shows dips in the spectra, the laser signal coming from the particle surface can increase or decrease on resonance, depending on how the speckle is aligned to the fiber. This explains the differing shapes of the signals in the experiments and the simulations. Fitting Fig. 4(c)(i) by a Gaussian curve, we deduce a width that is similar to the PL width of Fig. 4(b)(i) (2.1 and 2.8 G, respectively). This gives a width of 9 (12) MHz comparable to the inhomogeneous broadening of the sample. Similar experiments were realized on different particles under different degeneracies. In Sec. V of the SM, we present results taken under a twofold degeneracy.
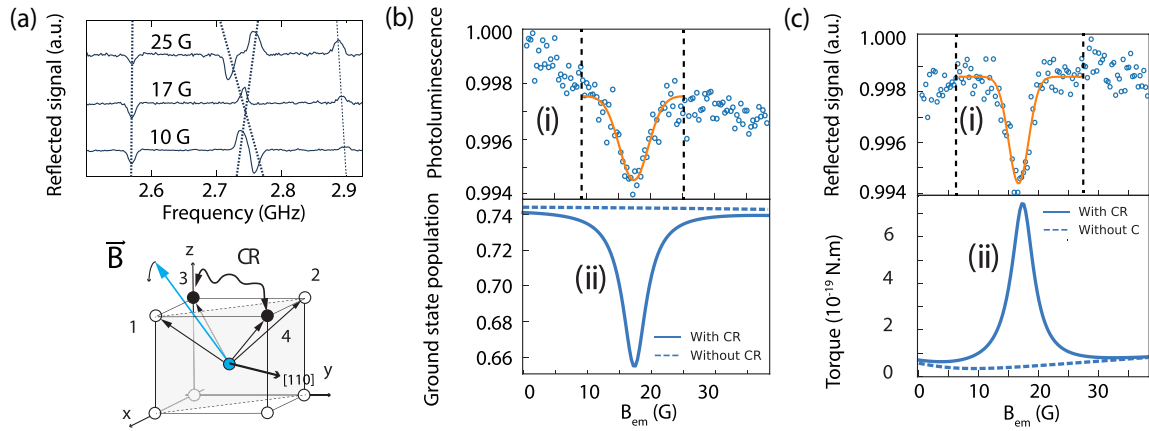
FIG. 4. (a) Top: Signal reflected off the diamond surface as a function of microwave frequency for three different magnetic field values. Bottom: Sketch showing the crossing of a crystal plane when the magnetic field angle is tuned. (b) PL detection as a function of B_{em} across a dipole-dipole resonance. (i) Experimental data with a Gaussian fit, and (ii) simulation of the population in $|m_s = 0\rangle$ state, taking into account (plain lines) or not (dashed lines) cross-relaxation. (c) Angular detection as a function of B_{em} across a resonance. (i) Experimental data with a Gaussian fit, and (ii) simulation of the magnetic torque applied to the diamond.

Let us conclude by mentioning two applications offered by dipole-dipole induced mechanical rotation. First, when performed under vacuum [44], this effect can be employed to control the temperature and stiffness of mechanical oscillators in the absence of a microwave. For cooling, a delay between the spin and Paul trap torques [1,10,45] will be introduced by tuning the polarizing laser power to reach a depolarizing rate (≈ 10 kHz) of the order of the trapping frequency. At a magnetic field value corresponding to a negative detuning from the CR feature, the NV fluctuator will depolarize a pair of spins and let the two other NV classes apply a torque until the previous pair repolarizes, extracting energy from the angular motion during each cooling cycle [46].

Conversely, the CR-induced torque can be viewed as another spectroscopic technique for sensing dipolar interactions between NV centers and spins that cannot be polarized optically. Using a magnetic field oriented close to the diamond [111] direction would, for instance, enable detection of dark paramagnetic species such the P_1 centers [22]. The method may open a path towards the, otherwise difficult, experimental investigations of angular momentum conservation during relaxation processes in crystals, as proposed in Ref. [23].

[1] M. Aspelmeyer, T. J. Kippenberg, and F. Marquardt, Rev. Mod. Phys. **86**, 1391 (2014).

[2] P. Treutlein, C. Genes, K. Hammerer, M. Poggio, and P. Rabl, Hybrid mechanical systems, in *Cavity Optomechanics: Nano- and Micromechanical Resonators Interacting with Light*, edited by M. Aspelmeyer, T. J. Kippenberg, and F. Marquardt (Springer, Berlin, 2014), pp. 327–351.

[3] P. Rabl, P. Cappellaro, M. V. Gurudev Dutt, L. Jiang, J. R. Maze, and M. D. Lukin, Phys. Rev. B **79**, 041302(R) (2009).

[4] D. Lee, K. W. Lee, J. V. Cady, P. Ovartchaiyapong, and A. C. B. Jayich, J. Opt. **19**, 033001 (2017).

[5] S. Bose, A. Mazumdar, G. W. Morley, H. Ulbricht, M. Toroš, M. Paternostro, A. A. Geraci, P. F. Barker, M. S. Kim, and G. Milburn, Phys. Rev. Lett. **119**, 240401 (2017).

[6] C. Wan, M. Scala, G. W. Morley, ATM. A. Rahman, H. Ulbricht, J. Bateman, P. F. Barker, S. Bose, and M. S. Kim, Phys. Rev. Lett. **117**, 143003 (2016).

[7] Y. Ma, T. M. Hoang, M. Gong, T. Li, and Z.-q. Yin, Phys. Rev. A **96**, 023827 (2017).

[8] S. Kolkowitz, A. C. Bleszynski Jayich, Q. P. Unterreithmeier, S. D. Bennett, P. Rabl, J. G. E. Harris, and M. D. Lukin, Science **335**, 1603 (2012).

[9] J. Gieseler, A. Kabcenell, E. Rosenfeld, J. D. Schaefer, A. Safira, M. J. A. Schuetz, C. Gonzalez-Ballestero, C. C. Rusconi, O. Romero-Isart, and M. D. Lukin, Phys. Rev. Lett. **124**, 163604 (2020).

[10] T. Delord, P. Huillery, L. Nicolas, and G. Hétet, Nature (London) **580**, 56 (2020).

[11] O. Arcizet, V. Jacques, A. Siria, P. Poncharal, P. Vincent, and S. Seidelin, Nat. Phys. **7**, 879 (2011).

[12] B.-B. Wei, C. Burk, J. Wrachtrup, and R.-B. Liu, EPJ Quantum Technol. **2**, 18 (2015).

[13] R. Bachelard, N. Piovella, and P. W. Courteille, Phys. Rev. A **84**, 013821 (2011).

[14] P. V. Panat and S. V. Lawande, Int. J. Mod. Phys. B **16**, 3787 (2002).

[15] B. Prasanna Venkatesh, M. L. Juan, and O. Romero-Isart, Phys. Rev. Lett. **120**, 033602 (2018).

[16] M. L. Juan, C. Bradac, B. Besga, M. Johnsson, G. Brennen, G. Molina-Terriza, and T. Volz, Nat. Phys. **13**, 241 (2017).

[17] E. van Oort and M. Glasbeek, Phys. Rev. B **40**, 6509 (1989).

[18] S. Armstrong, L. J. Rogers, R. L. McMurtrie, and N. B. Manson, Phys. Proc. **3**, 1569 (2010).

[19] N. Alfasi, S. Masis, O. Shtempluck, and E. Buks, Phys. Rev. B **99**, 214111 (2019).

[20] R. J. Epstein, F. M. Mendoza, Y. K. Kato, and D. D. Awschalom, Nat. Phys. **1**, 94 (2005).

[21] L. T. Hall, P. Kehayias, D. A. Simpson, A. Jarmola, A. Stacey, D. Budker, and L. C. L. Hollenberg, Nat. Commun. **7**, 10211 (2016).

[22] H.-J. Wang, C. S. Shin, C. E. Avalos, S. J. Seltzer, D. Budker, A. Pines, and V. S. Bajaj, Nat. Commun. **4**, 1940 (2013).

[23] P. R. Zangara, A. Wood, M. W. Doherty, and C. A. Meriles, Phys. Rev. B **100**, 235410 (2019).

[24] A. Abragam, *The Principles of Nuclear Magnetism; Reprint with Corrections*, International Series of Monographs on Physics (Clarendon, Oxford, UK, 1989).

[25] See Supplemental Material at http://link.aps.org/supplemental/10.1103/PhysRevB.104.L100411 for futher experimental and theoretical details, which includes Refs. [17,26–34].

[26] T. Delord, P. Huillery, L. Schwab, L. Nicolas, L. Lecordier, and G. Hétet, Phys. Rev. Lett. **121**, 053602 (2018).

[27] T. Delord, Spin-mechanics with micro-particles levitating in a Paul trap, Ph.D. thesis, École Normale Supérieure, 2019.

[28] J. R. Johansson, P. D. Nation, and F. Nori, Comput. Phys. Commun. **183**, 1760 (2012).

[29] J. Johansson, Comput. Phys. Commun. **184**, 1234 (2013).

[30] J. Choi, S. Choi, G. Kucsko, P. C. Maurer, B. J. Shields, H. Sumiya, S. Onoda, J. Isoya, E. Demler, F. Jelezko, N. Y. Yao, and M. D. Lukin, Phys. Rev. Lett. **118**, 093601 (2017), number: 9.

[31] A. Jarmola, V. M. Acosta, K. Jensen, S. Chemerisov, and D. Budker, Phys. Rev. Lett. **108**, 197601 (2012).

[32] A. Jarmola, A. Berzins, J. Smits, K. Smits, J. Prikulis, F. Gahbauer, R. Ferber, D. Erts, M. Auzinsh, and D. Budker, Appl. Phys. Lett. **107**, 242403 (2015).

[33] R. Akhmedzhanov, L. Gushchin, N. Nizov, V. Nizov, D. Sobgayda, I. Zelensky, and P. Hemmer, Phys. Rev. A **96**, 013806 (2017).

[34] R. Akhmedzhanov, L. Gushchin, N. Nizov, V. Nizov, D. Sobgayda, I. Zelensky, and P. Hemmer, Phys. Rev. A **100**, 043844 (2019).

[35] K. Holliday, N. B. Manson, M. Glasbeek, and E. v. Oort, J. Phys.: Condens. Matter **1**, 7093 (1989).

[36] M. Mrózek, D. Rudnicki, P. Kehayias, A. Jarmola, D. Budker, and W. Gawlik, EPJ Quantum Technol. **2**, 22 (2015).

[37] C. Pellet-Mary, P. Huillery, M. Perdriat, A. Tallaire, and G. Hétet, Phys. Rev. B **103**, L100411 (2021).

[38] N. B. Manson, M. Hedges, M. S. J. Barson, R. Ahlefeldt, M. W. Doherty, H. Abe, T. Ohshima, and M. J. Sellars, New J. Phys. **20**, 113037 (2018).

[39] J.-P. Tetienne, T. Hingant, L. Rondin, A. Cavaillès, L. Mayer, G. Dantelle, T. Gacoin, J. Wrachtrup, J.-F. Roch, and V. Jacques, Phys. Rev. B **87**, 235436 (2013).

[40] S. Dhomkar, H. Jayakumar, P. R. Zangara, and C. A. Meriles, Nano Lett. **18**, 4046 (2018).

[41] R. Giri, C. Dorigoni, S. Tambalo, F. Gorrini, and A. Bifone, Phys. Rev. B **99**, 155426 (2019).

[42] R. Giri, F. Gorrini, C. Dorigoni, C. E. Avalos, M. Cazzanelli, S. Tambalo, and A. Bifone, Phys. Rev. B **98**, 045401 (2018).

[43] D. Rugar, R. Budakian, H. J. Mamin, and B. W. Chui, Nature (London) **430**, 329 (2004).

[44] T. Delord, L. Nicolas, M. Bodini, and G. Hétet, Appl. Phys. Lett. **111**, 013101 (2017).

[45] M. Perdriat, C. Pellet-Mary, P. Huillery, L. Rondin, and G. Hétet, Micromachines **12**, 651 (2021).

[46] V. B. Braginskiĭ and A. B. Manukin, Sov. Phys. - JETP **25**, 653 (1967).